Supporting Information

Low-temperature suitability of flexible photo-rechargeable devices integrated with hydrogel-based lithium-ion battery and perovskite solar cell

Wei Liu[a,1], Mingzhu He[a,1], Hai Lu[a], Hai Zhong[a,*], Ziwei Cai[a], Shaohang Wu[a,*], Yingxiang Tan[a], Xingjiang Liu[b,*], and Yaohua Mai[a,c]

[a] Institute of New Energy Technology, College of Physics and Optoelectronic Engineering, Jinan University, Guangzhou 510006, China

[b] National Key Laboratory of Chemical and Physical Power Sources, Tianjin Institute of Power Sources, Tianjin300384, P. R. China

[c] Guangdong Mellow Energy Co., Ltd, Guangzhou 510630, China

[1] Wei Liu and Mingzhu He have contributed equally to this work.

*Corresponding author E-mail: haizhong@jnu.edu.cn (H. Zhong), shaohangwu@jnu.edu.cn (S. H. Wu), xjliu@nklps.orgs (X. J. Liu)

Fig. S1 XRD spectra of PCPL film, PAE:CMC:PAM (3:2:1) film, and $LiNO_3$ powders.

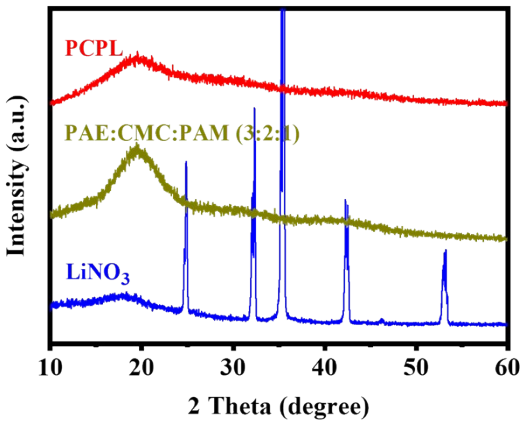

Fig. S2 FTIR of PCPL film, $LiNO_3$ powders, CMC powders, PAE film, and PAM powders.

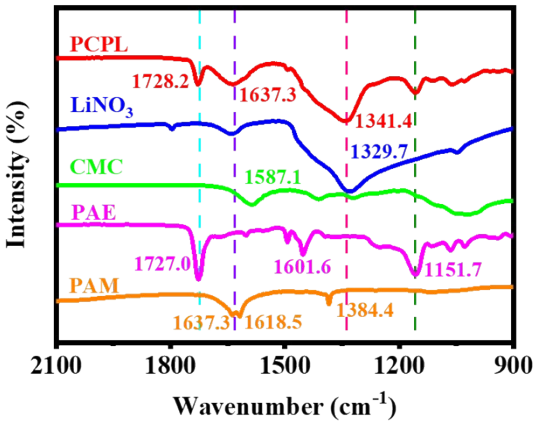

Fig. S3 Stress-strain curve of PCPL film.

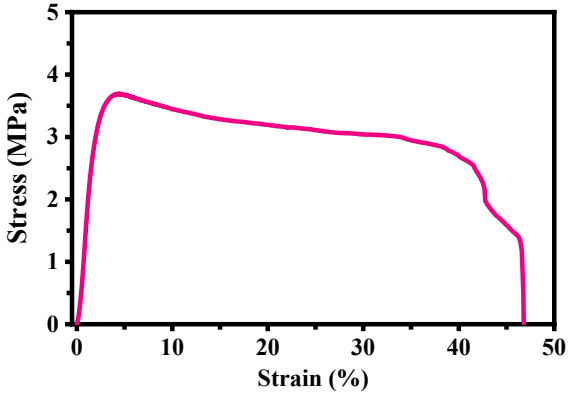

Fig. S4 EIS curve of PCPL film and the calculated ionic conductivity was obtained at −20 °C.

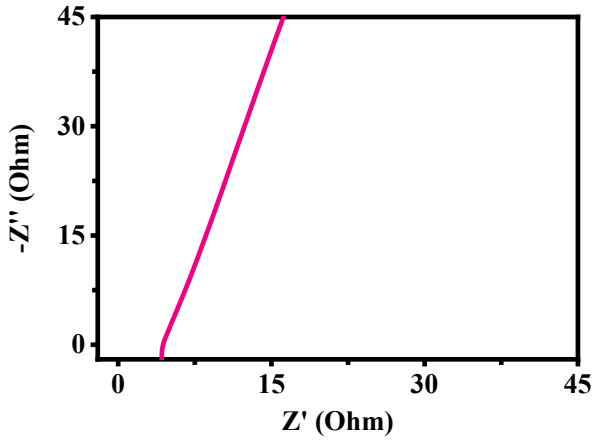

Fig. S5 The bending property of the hydrogel-based electrolyte at −20 °C.

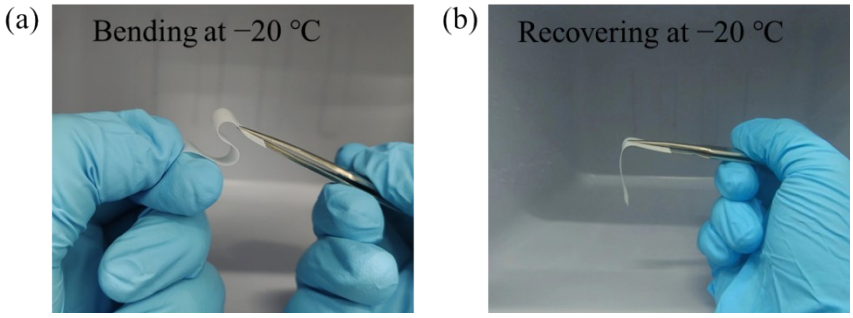

Fig. S6 Photography of HE-LIB (a) top view is anode side; (b) top view is cathode side.

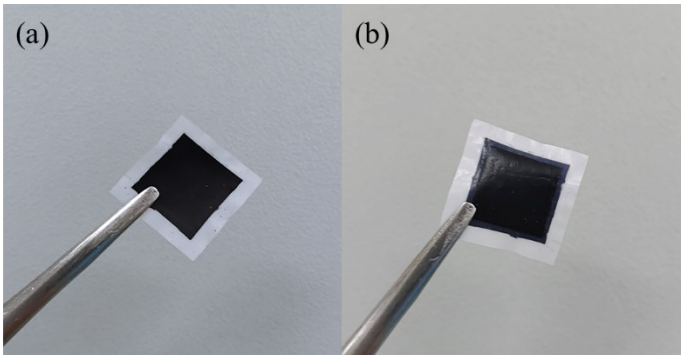

Fig. S7 Corresponding voltage–capacity profiles at selected cycles in Fig. 2d.

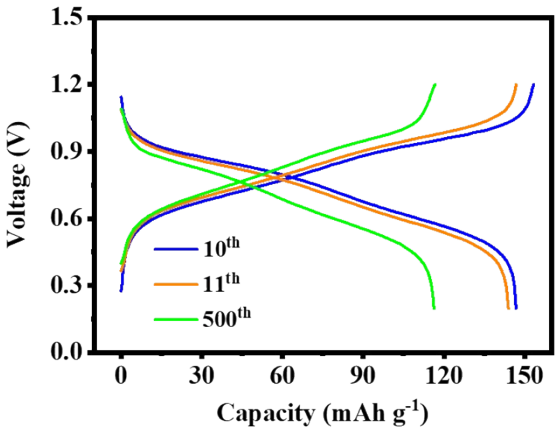

Fig. S8 (a) Corresponding voltage–capacity profiles at current densities ranging from 0.5C to 5C in Fig. 2e; (b) Corresponding energy density and ESE (as calculated by the weight of $LiFePO_4$) at various C-rates.

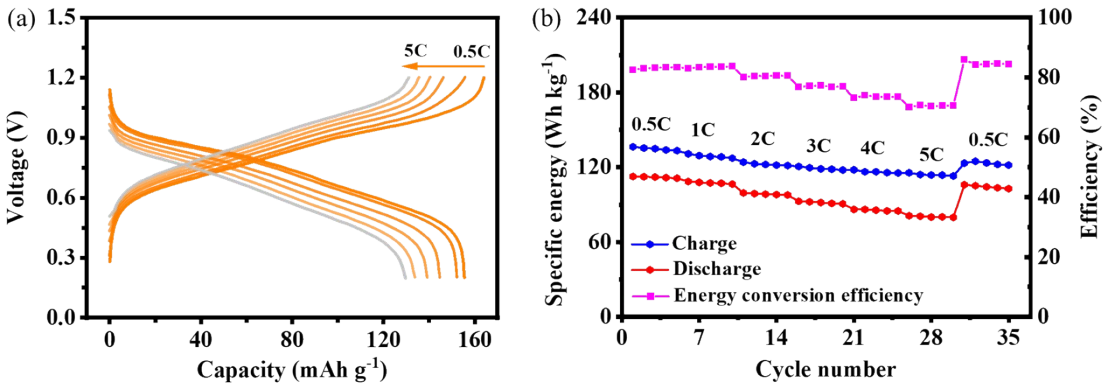

Fig. S9 Photography of *f*-PSC with area 0.12 cm^2 (a) flat state; (b) bend state.

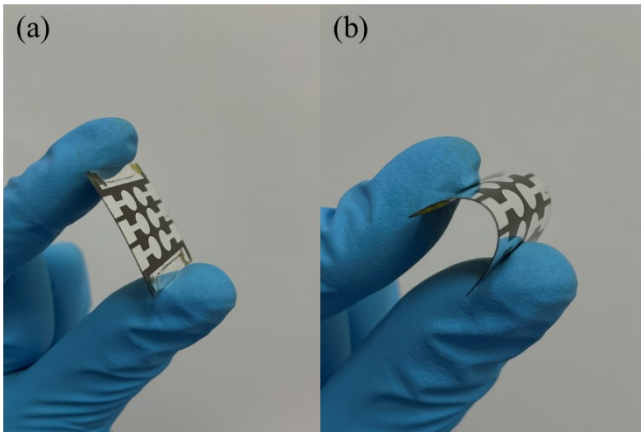

Table S1 Comparison of η_{OEE} with a recently reported photo-rechargeable device.

	OEE	**PCE**	**Energy storage device**	**Photovoltaic cells**	Ref.
1	5.28%	16.6%	Zn-MnO_2 micro-battery	Flexible perovskite solar cells	[1]
2	11.2%	25.0%	All-solid-state Li-S battery	Perovskite solar cells	[2]
3	12.04%	18.5%	Aluminum-ion battery	Perovskite solar cells	[3]
4	5.14%	15.9%	Non-aqueous Li-S battery	Perovskite solar cells	[4]
5	9.3%	16.8%	Aqueous Li/Na-ion battery	Perovskite solar cells	[5]
6	6.4%	14.85%	Rechargeable zinc battery	Perovskite solar cells	[6]
7	12.88%	21.48%	Quasi-solid-state Li-ion battery	Flexible perovskite solar cells	This work

Fig. S10 The corresponding voltage–capacity profiles of HE-LIB in Fig. 4b.

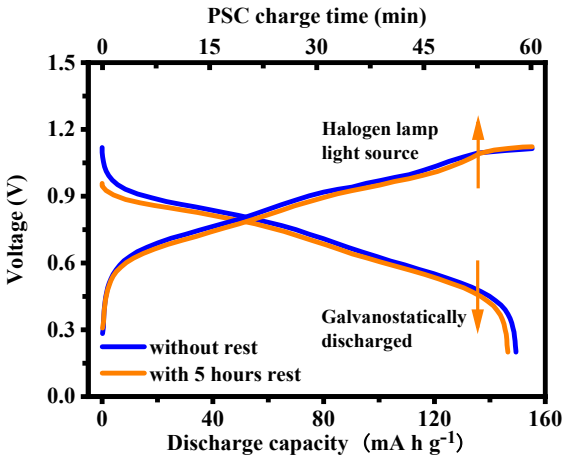

Fig. S11 Effect of the photo-rechargeable device without an antireverse charging circuit.

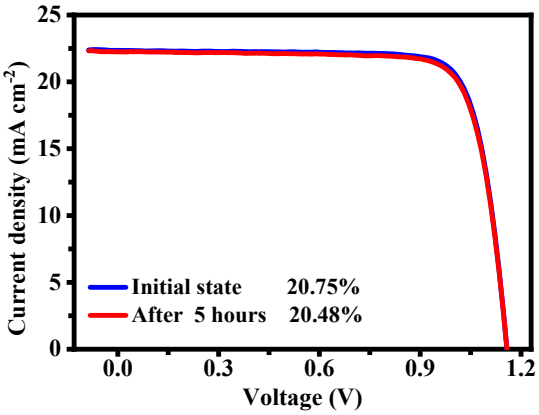

Fig. S12 The corresponding galvanostatically discharge profile of the HE-LIB unit in photo-rechargeable device under light condition at 0, 6, 12, and 24 hours.

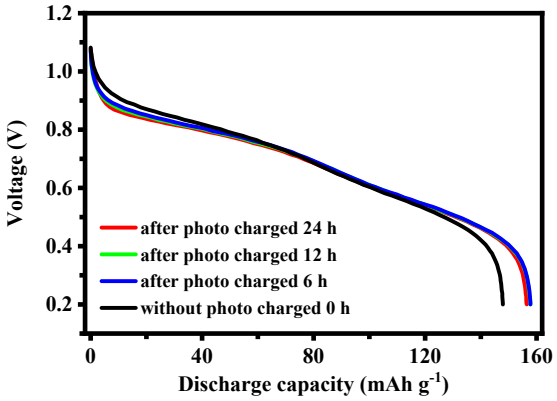

Table S2 The corresponding photovoltaic parameters of encapsulated *f*-PSC in Fig. 4c.

	PCE (%)	V_{OC} (%)	J_{SC} (mA cm^{-2})	FF(%)
Without rest	20.75	1.15	22.35	80.92
With 5 h rest	20.48	1.15	22.27	80.15

Fig. S13 Corresponding voltage–capacity profiles at 5th (25 °C), 11th (−20 °C), and 55th (−20 °C) in Fig. 4f.

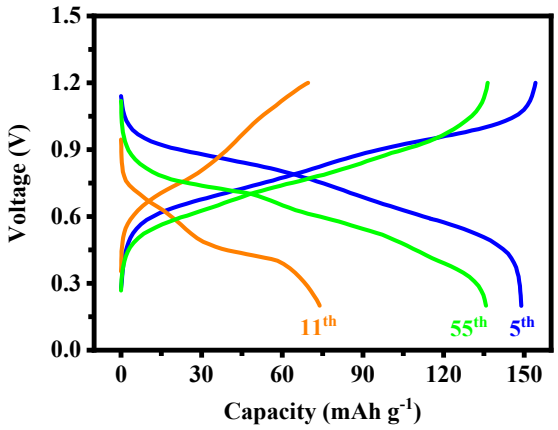

Fig. S14 Cyclic stability of flexible HE-LIB at initial state and bending state (with a curvature radius of ~ 1 mm).

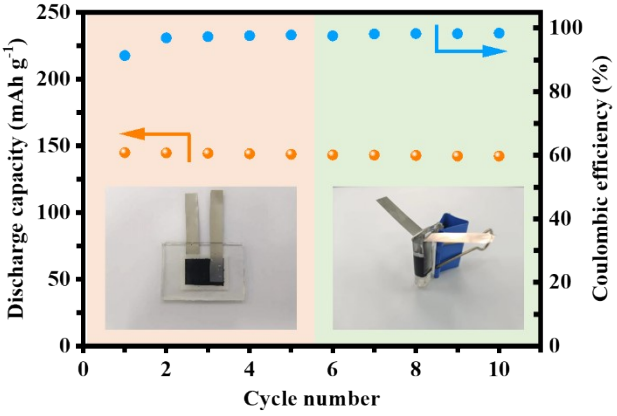

Fig. S15 *J-V* curves and photovoltaic parameters of *f*-PSC under different bending states.

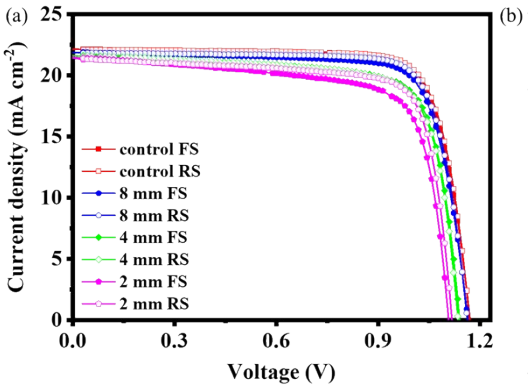

(b)

Bend radius (mm)		PCE (%)	*Voc* (V)	*Jsc* (mA cm^{-2})	FF (%)
control	FS	20.38	1.1610	22.15	79.24
	RS	20.63	1.1608	22.12	80.33
8	FS	19.86	1.1607	21.86	78.28
	RS	20.24	1.1608	21.83	79.87
4	FS	18.53	1.1344	21.57	75.71
	RS	18.65	1.1345	21.63	76.00
2	FS	17.27	1.1093	21.44	73.49
	RS	18.43	1.0961	21.39	77.68

Fig. S16 Photography of photo-rechargeable device integrated by flexible HE-LIB unit and *f*-PSC unit.

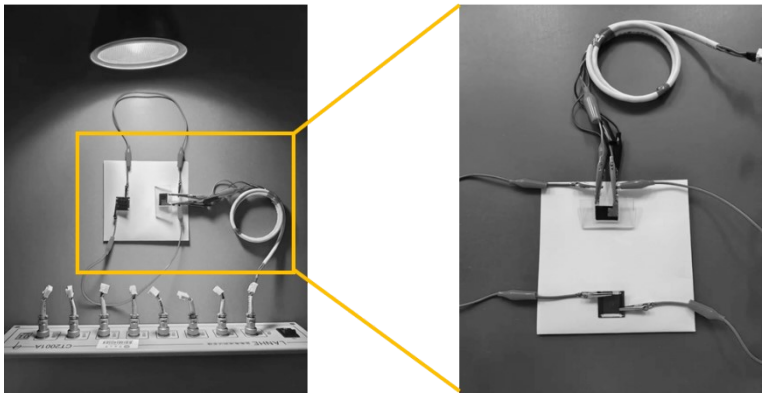

Fig. S17 Photography of *f*-PSC with an area of 1.00 cm^2.

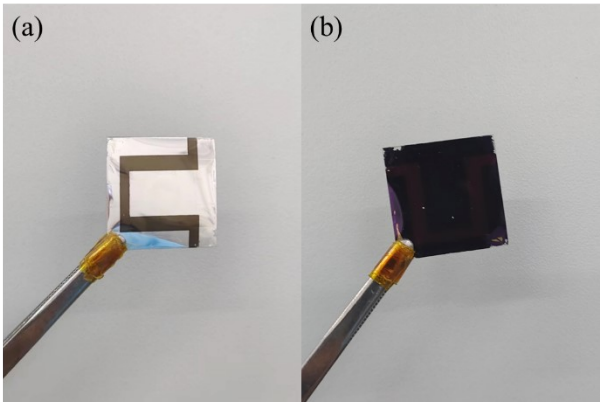

Fig. S18 *J-V* curves and photovoltaic parameters of *f*-PSC with an area of 1.00 cm^2 under (a) initial state and (b) after 10 bending cycles state (bend radius is 4 mm).

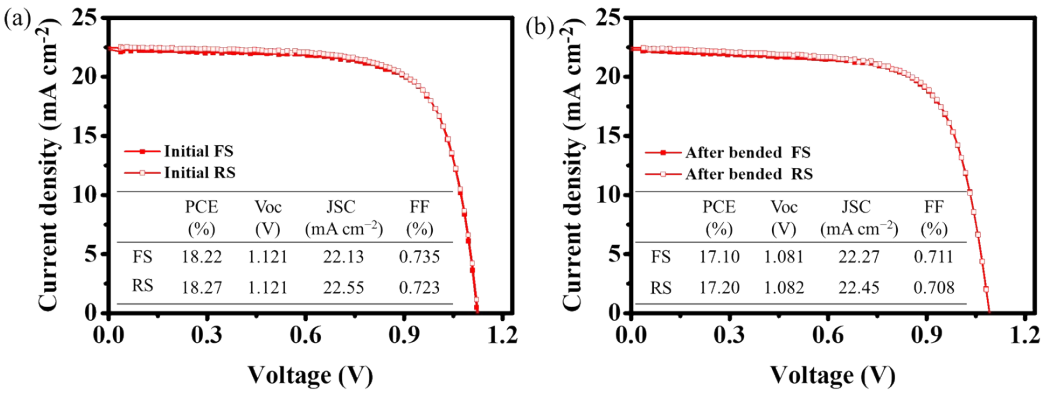

Reference:

[1] J. Bi, J. Zhang, P. Giannakou, T. Wickramanayake, X. Yao, M. Wang, X. Liu, M. Shkunov, W. Zhang, Y. Zhao, A highly integrated flexible photo-rechargeable system based on stable ultrahigh-rate quasi-solid-state zinc-ion micro-batteries and perovskite solar cells, Energy Storage Materials, 51 (2022) 239-248.

[2] T. Li, Y. Yang, B. Zhao, Y. Wu, X. Wu, P. Chen, X. Gao, Photo-rechargeable all-solid-state lithium-sulfur batteries based on perovskite indoor photovoltaic modules, Chemical Engineering Journal, 455 (2023) 140684.

[3] Y. Hu, Y. Bai, B. Luo, S. Wang, H. Hu, P. Chen, M. Lyu, J. Shapter, A. Rowan, L. Wang, A portable and efficient solar-rechargeable battery with ultrafast photo-charge/discharge rate, Advanced Energy Materials, 9 (2019) 1900872.

[4] P. Chen, G.R. Li, T.T. Li, X.P. Gao, Solar-driven rechargeable lithium-sulfur battery, Advanced Science, 6 (2019) 1900620.

[5] G. Weng, J. Kong, H. Wang, C. Karpovich, J. Lipton, F. Antonio, Z.S. Fishman, H. Wang, W. Yuan, A.D. Taylor, A highly efficient perovskite photovoltaic-aqueous Li/Na-ion battery system, Energy Storage Materials, 24 (2020) 557-564.

[6] P. Chen, T. Li, Y. Yang, G. Li, X. Gao, Coupling aqueous zinc batteries and perovskite solar cells for simultaneous energy harvest, conversion and storage, Nature Communications, 13 (2022) 64.